Supporting information

Simultaneous Promotion of Lattice Oxygen Mechanism and Chloride Resistance *via* Iron Doping in Cobalt Sulfide toward Robust Seawater Splitting

Huijun Zhu[a], Zekai Zhu[a], Yuying Meng[*a,b], Lei Feng[a], Bing Du[c], Wenbiao Zhang[a], Qingsheng Gao[*a]

a College of Chemistry and Materials Science, Jinan University, Guangzhou 510632, China

b Institute of Advanced Wear & Corrosion Resistant and Functional Materials, Jinan University, Guangzhou, 510632, China

c *College of Materials Science and Engineering, Shenzhen University, 1066 Xueyuan Avenue, Shenzhen, 518060, China*

Corresponding author: Yuying Meng (yymeng9169@jnu.edu.cn)

Qingsheng Gao (tqsgao@jnu.edu.cn)

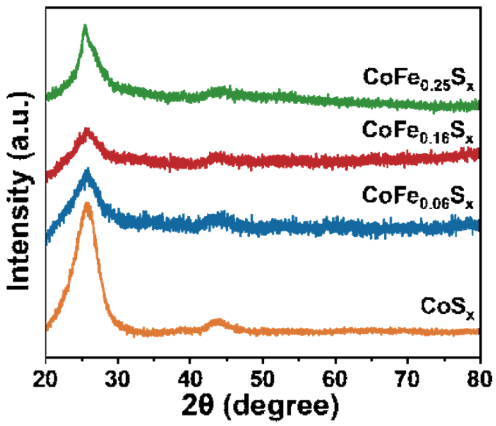

Figure S1 XRD patterns of CoS_x, $CoFe_{0.06}S_x$, $CoFe_{0.16}S_x$, and $CoFe_{0.25}S_x$.

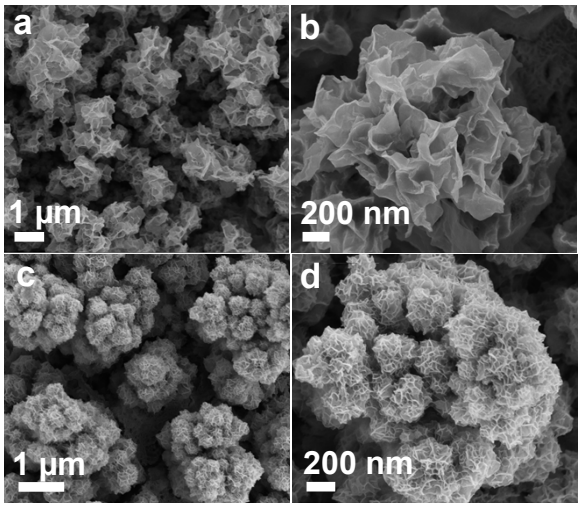

Figure S2 SEM images of (a,b) $CoFe_{0.06}S_x$ and (c,d) $CoFe_{0.25}S_x$.

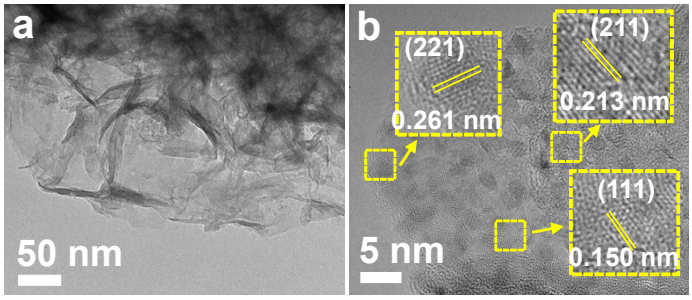

Figure S3 (a) TEM image of CoS_x. (b) HRTEM image of CoS_x.

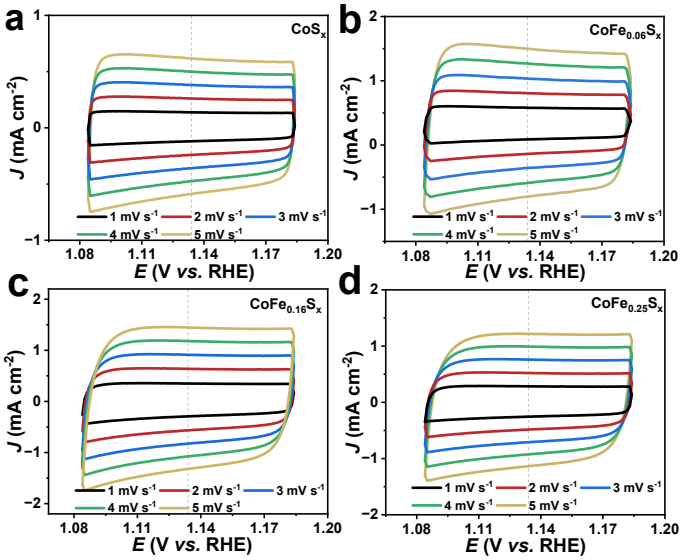

Figure S4 Cyclic voltammograms at various scan rates of 1, 2, 3, 4, and 5 mV s^{-1} for (a) CoS_x, (b) $CoFe_{0.06}S_x$, (c) $CoFe_{0.16}S_x$, and (d) $CoFe_{0.25}S_x$.

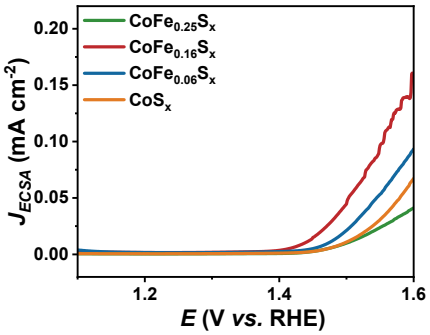

Figure S5 LSV curves with the current density normalized by ECSA over CoS_x-based electrodes in 1.0 M KOH solution.

v

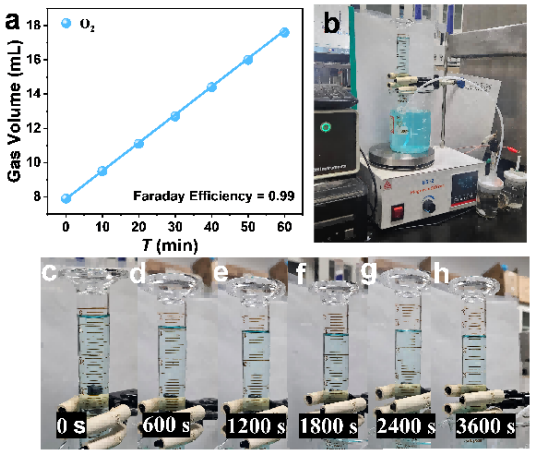

Figure S6 (a) Measured and calculated volume of O_2 as a function time. (b) Diagram of the Faraday efficiency test device. (c-h) The digital photograph of O_2 volume collected at different time (0 s, 600 s, 1200 s, 1800 s, 2400 s, 3600 s).

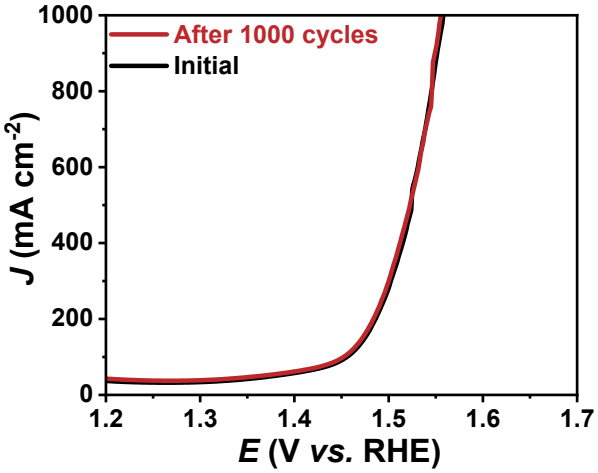

Figure S7 LSV curves before and after 1000 cycles continues test.

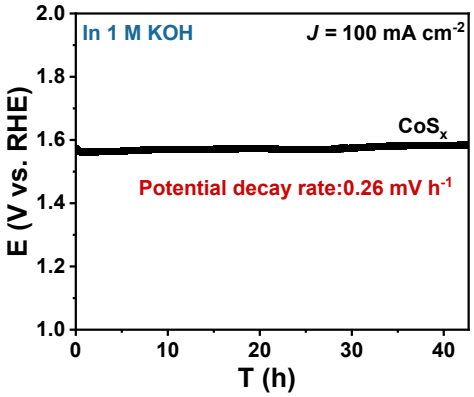

Figure S8 Chronopotentiometric measurements conducted at 1.0 M KOH under a current density of 100 mA cm^{-2}.

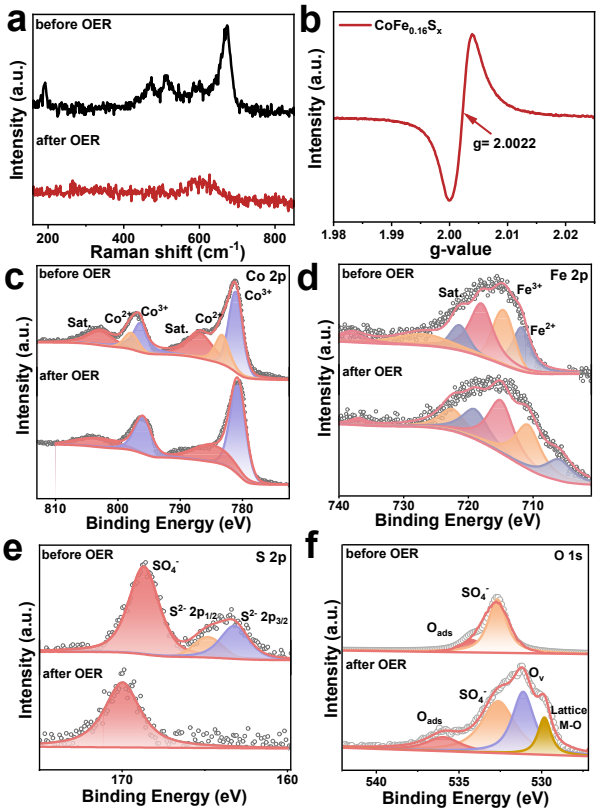

Figure S9 (a) Raman spectra of $CoFe_{0.16}S_x$ before and after 94 h long-term stability test toward OER at 100 mA cm^{-2}. (b) EPR spectrum of $CoFe_{0.16}S_x$ after 1000CV activation in 1 M KOH. High-resolution spectra for (c) Co 2p (d) Fe 2p (e) S 2p and (f) O 1s in $CoFe_{0.16}S_x$ before and after 94 h long-term stability test toward OER at 100 mA cm^{-2}.

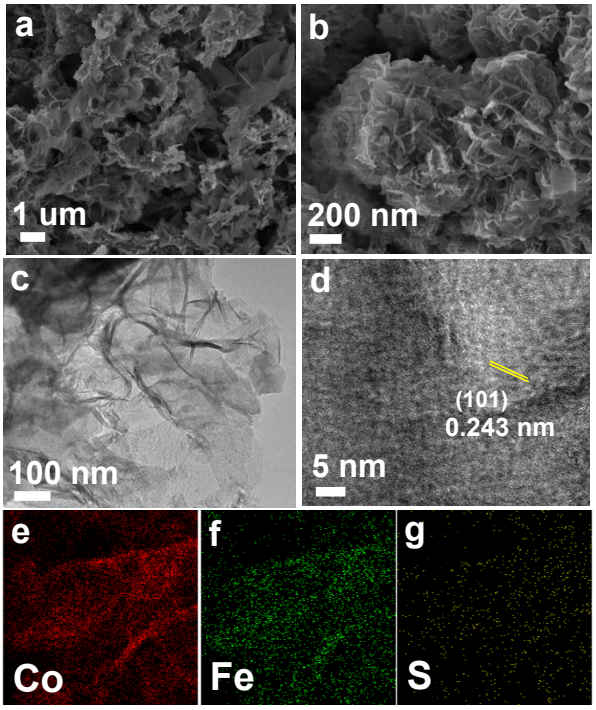

Figure S10 Morphological information of Fe-CoS_x after 94 h long-term stability test toward OER at 100 mA cm^{-2}. (a,b) SEM and (c,d) TEM. (e-g) EDS elemental mapping images of $CoFe_{0.16}S_x$ after OER.

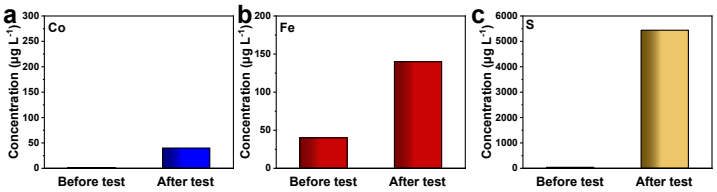

Figure S11 ICP-MS analysis of the post-reaction electrolyte. (a) Co, (b) Fe, and (c) S.

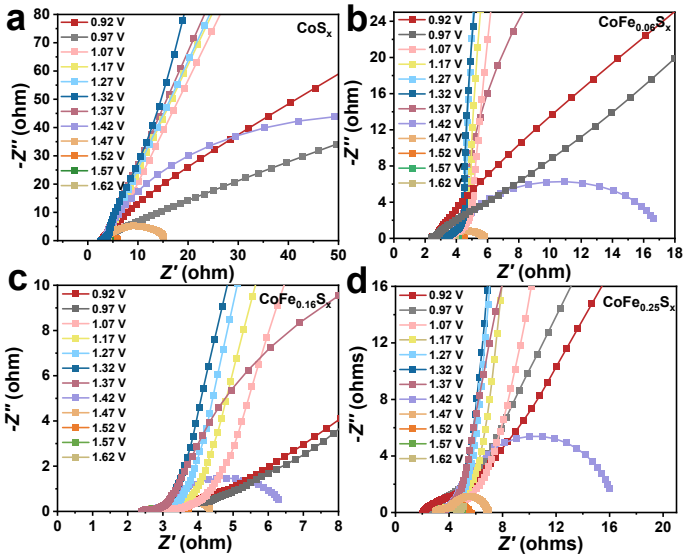

Figure S12 EIS plots at different potentials of (a) CoS_x, (b) $CoFe_{0.06}S_x$, (c) $CoFe_{0.16}S_x$, and (d) $CoFe_{0.25}S_x$.

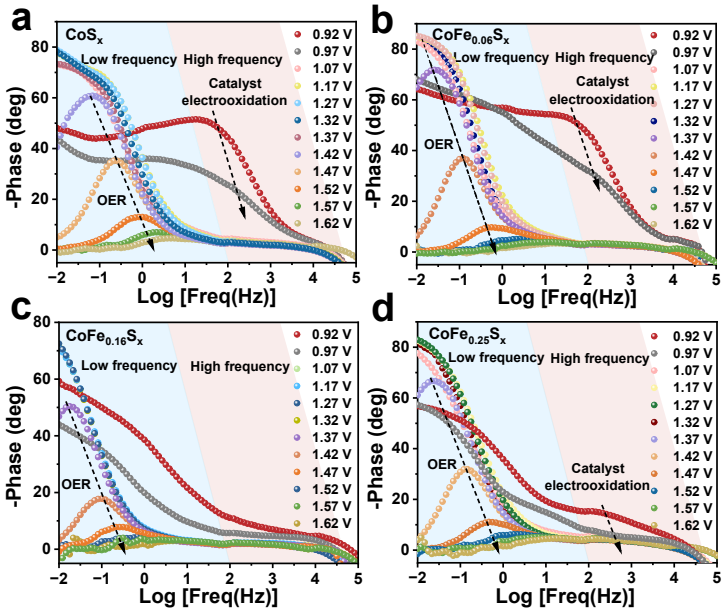

Figure S13 *In-situ* Bode phase plots under different potentials (from 0.92 to 1.62 V) for (a) CoS_x, (b) $CoFe_{0.06}S_x$, (c) $CoFe_{0.16}S_x$, and (d) $CoFe_{0.25}S_x$.

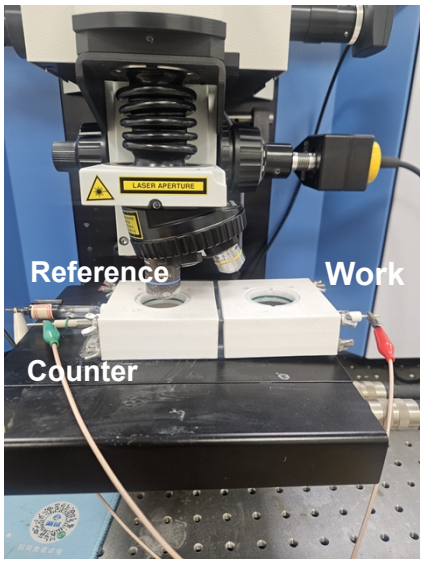

Figure S14 Images of *in situ* Raman setup.

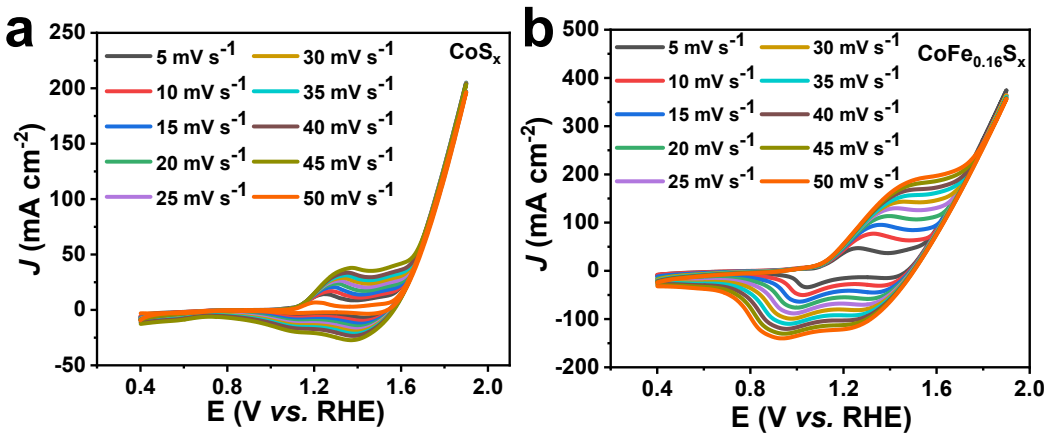

Figure S15 CVs of (a) CoS_x and (b) $CoFe_{0.16}S_x$ at different scan rates increasing from 5 to 50 mV s^{-1} in 1.0 M KOH.

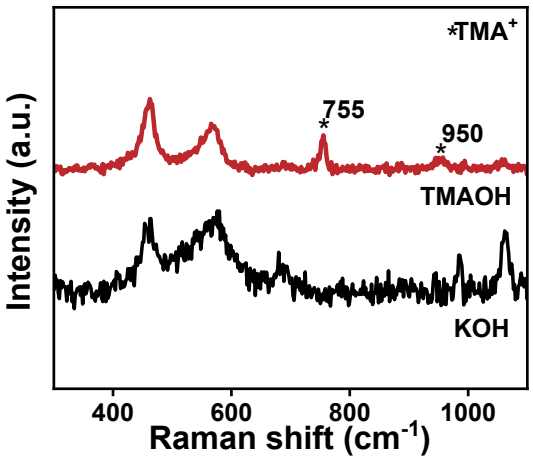

Figure S16 Raman spectra of $CoFe_{0.16}S_x$ after test in TMAOH.

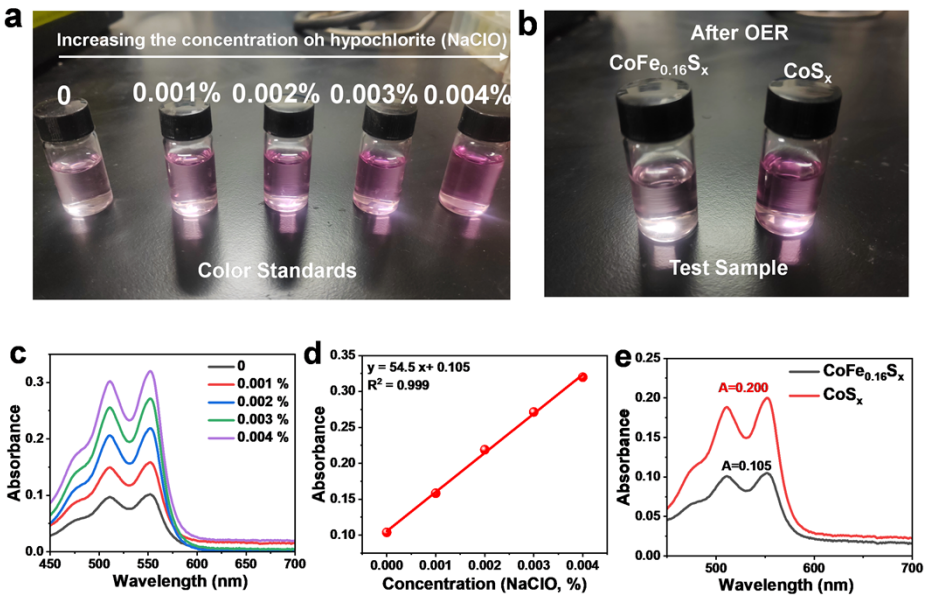

Figure S17 (a) The digital photograph of the electrolyte hypochlorite detection result for 1 M KOH + 0.5 M NaCl with different NaClO contents. (b) After 124 h electrolysis for $CoFe_{0.16}S_x$ and CoS_x at 100 mA cm^{-2} in 1 M KOH + 0.5 M NaCl. (c) UV-vis absorption spectra of ClO^- with different concentrations. (d) Calibration curve used for calculating ClO^- concentrations of the electrolyte and (f) UV-vis absorption spectrum of the electrolyte after 124 h electrolysis for $CoFe_{0.16}S_x$ and CoS_x at 100 mA cm^{-2} in 1 M KOH + 0.5 M NaCl.